Research on Modeling and Simulation of the Primary Coolant System for China Experimental Fast Reactor

Zhijian Zhang, Zhigang Zhang*, Guangliang Chen, Yang Yu

Fundamental Science on Nuclear Safety and Simulation Technology Laboratory, Harbin Engineering University, Harbin, China

**zg_zhang@hrbeu.edu.cn*

Abstract. Based on the structure and physical characteristics of primary coolant system (PCS) of China Experimental Fast Reactor (CEFR), a series of reasonable mathematical and physical models were set up. A set of stable and highly effective numerical methods were used to solve the models. Then the real-time thermal-hydraulic analysis codes for PCS of CEFR have been developed with the modular method by using FORTRAN programming language. The codes have been merged into SimExecTM real-time simulation platform and linked to the modules of other systems.

The models include the basic thermal-hydraulic model of coolant, the heat transfer model of fuel pellet, the heat thermal model of intermediate heat exchangers (IHX), the model of primary pump, the flow friction and heat transfer correlations, the thermo-physical properties, etc. "Control body" method was put forward in the set of models and Gear method was applied to solve the thermal-hydraulic model of coolant and heat transfer model of fuel pellet. Quasi-newton iteration method was used to solve the flow rate distribution equations. The model and numerical method in this research contribute to the accuracy and effectiveness of the calculation to meet the requirement of real-time simulation.

The design parameters of CEFR were used to validate six different steady-state conditions from 26.5%FP to 100%FP by this code, and the steady-state calculation of the reactor main vessel cooled system was also finished and the results were compared with the datum obtained by the references. Thus the validity and applicability of this code was proved. The normal operation conditions were calculated and validated by the manual of PCS of CEFR. The reactivity insertion accident, the loss of coolant accident and the loss of heat sink accident were also simulated. The results showed that the trend of simulation curves for the steady and transient conditions are reasonable, which are in accordance with the actual physical process. The real-time characteristics of the code were analyzed and could meet the simulation requirements.

Key Words: CEFR, PCS, real time, simulation.

1 Introduction

China experimental fast reactor (CEFR) is the first sodium-cooled fast reactor in China. A transient analysis code is urgently needed to ensure its safe operation and for training operators, and this code will also help the designers and engineers in the development of China Demonstration Fast Reactor. The abilities for simulating the normal operations and accident conditions and the accuracy for the simulation are both important for the operation and training, and the computing efficiency is also important for the training. Therefore these significant features are necessary to be considered for the developing code.

There were some research work for the modeling of several fast reactors, such as: IANUS code [1] for the Fast Reactor Test Facility, DEMO [2] for the Clinch River Breeder Reactor, and NATDEMO [3] for the EBR-II. The major drawback of these codes is that the physical models, the mathematical models and the numerical algorithm are coupled so tight for the special reactor that these codes cannot be used without significant modifications for a new sodium

cooled fast reactor. Therefore the modularized modes for the simulation of CEFR are needed and the modularized modes must be easy to modify and expand for the code update in the future.

The simulation of loop type fast reactors is more mature compared with pool type reactors. For instance, SSC-L [4], SSC-K [5,6] and DINROS are just this kind codes. DINROS is a system code developed for the transient and event process analysis, and this code has been applied in the initial safety analysis report for CEFR. But the code is still with some drawbacks: 1) the code is designed for the loop structure, not pool structure; 2) the heat transfer model for sodium pool is not in this code, but this physical process is crucial for the thermal inertia of the pools with total mass of 260 t; 3) The hottest channel and point cannot be found by this code. A work for the improvement of DINROS to eliminate the problems has been done and the new code has been used in the final analysis report, but the foundation of this code is still the old code, so the computer quality is not simplified, and the real-time simulation ability could not be obtained.

The purpose of this research is to develop a code based on the characteristics of the sodium-cooled pool type fast reactor with the advantages in accuracy and speed, suitable for the real-time simulation of normal and accident process for CEFR.

2 Physical Status and Simulation Schemes

In the development of this code, firstly the physical and mathematical model for the heat transfer and flow process of CEFR were analyzed, and the numerical methods were chosen and designed. Then the code based on the physical and mathematical model, and numerical method has been compiled and debugged in the PC environment. Then this code was transformed into the new format used in the SimExec and established the linkage with other system codes.

2.1.Flow Status and Models

In CEFR, the details of the main flow status of PCS can be seen from *FIG. 1*. There are two parallel circuit loops. Each loop is with two intermediate heat exchangers (IHX) and one vertical immersion-type centrifugal pump. The IHX and the pump link the hot and cold sodium pools together in each loop. The pump takes the cold sodium from the cold pool, and it sends the cold sodium to the pressure chamber. Then the liquid sodium flows into three flow paths. In the first path, the liquid sodium flows through the assemblies of the core and radial breeder region. In the secondary path, part sodium goes to cool the reactor vessel. In the third path, the remaining sodium cools the ionization chamber, pump components, etc. Based on these three paths, the cold sodium obtain higher temperature, and most sodium arrives at the hot pool. Then the hot sodium flows through the two IHXes of each loop. After the heat release in IHX, the temperature is reduced and the sodium arrives at the cold pool.

The flow distribution of CEFR core are decided by the pressure of some key locations, they

are: the argon region for system pressure boundary P_{pool} which is decided by the overpressure protection system; the grid plate region with pressure P_0 for the mixture of two circuits; The region with pressure P_{11} for the bottom of cold pool - first part; The region with pressure P_{12} for the bottom of cold pool - second part; The region with pressure P_{21} for the inlet region of pump support cooled system and pressure tube of PCS loop-1; The region with pressure P_{22} for the inlet region of pump support cooled system and pressure tube of PCS loop-2. The relation of these flows and positions are shown in FIG. *1* and FIG. 2. Then these pressures above and the mass flows can be solved by the momentum and mass conservation equations as Eq. 1 and Eq. 2.

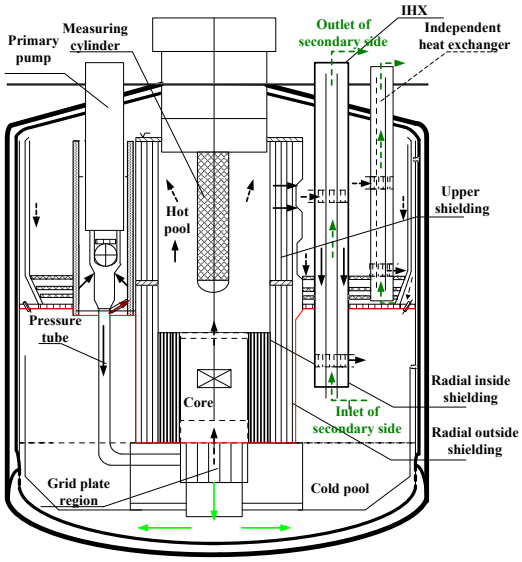

FIG. 1. The pool structure and flow status of CEFR

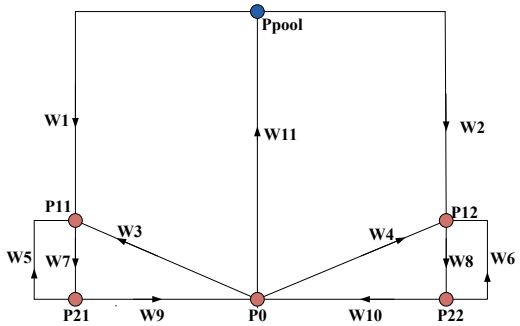

FIG. 2. The key flow distribution of CEFR

$$
\begin{cases}
\dfrac{L_1}{A_1}\dfrac{\partial W_1}{\partial t} = P_{pool} - P_{11} - \int_{l1}\dfrac{\partial}{\partial z}\left(\dfrac{W_1^2}{\rho A_1^2}\right)dz - \int_{l1}\dfrac{fW_1^2}{2D_e\rho A_1^2}dz - \int_{l1}\rho g dz - \sum_M \dfrac{\xi W_1^2}{2\rho A_1^2} \\
\dfrac{L_2}{A_2}\dfrac{\partial W_2}{\partial t} = P_{pool} - P_{12} - \int_{l2}\dfrac{\partial}{\partial z}\left(\dfrac{W_2^2}{\rho A_2^2}\right)dz - \int_{l2}\dfrac{fW_2^2}{2D_e\rho A_2^2}dz - \int_{l2}\rho g dz - \sum_M \dfrac{\xi W_2^2}{2\rho A_2^2} \\
\dfrac{L_3}{A_3}\dfrac{\partial W_3}{\partial t} = P_0 - P_{11} - \int_{l3}\dfrac{\partial}{\partial z}\left(\dfrac{W_3^2}{\rho A_3^2}\right)dz - \int_{l3}\dfrac{fW_3^2}{2D_e\rho A_3^2}dz - \int_{l3}\rho g dz - \sum_M \dfrac{\xi W_3^2}{2\rho A_3^2} \\
\dfrac{L_4}{A_4}\dfrac{\partial W_4}{\partial t} = P_0 - P_{12} - \int_{l4}\dfrac{\partial}{\partial z}\left(\dfrac{W_4^2}{\rho A_4^2}\right)dz - \int_{l4}\dfrac{fW_4^2}{2D_e\rho A_4^2}dz - \int_{l4}\rho g dz - \sum_M \dfrac{\xi W_4^2}{2\rho A_4^2} \\
\dfrac{L_5}{A_5}\dfrac{\partial W_5}{\partial t} = P_{21} - P_{11} - \int_{l5}\dfrac{\partial}{\partial z}\left(\dfrac{W_5^2}{\rho A_5^2}\right)dz - \int_{l5}\dfrac{fW_5^2}{2D_e\rho A_5^2}dz - \int_{l5}\rho g dz - \sum_M \dfrac{\xi W_5^2}{2\rho A_5^2} \\
\vdots \\
\dfrac{L_{11}}{A_{11}}\dfrac{\partial W_{11}}{\partial t} = P_0 - P_{pool} - \int_{l11}\dfrac{\partial}{\partial z}\left(\dfrac{W_{11}^2}{\rho A_{11}^2}\right)dz - \int_{l11}\dfrac{fW_{11}^2}{2D_e\rho A_{11}^2}dz - \int_{l11}\rho g dz - \sum_M \dfrac{\xi W_{11}^2}{2\rho A_{11}^2}
\end{cases}
\quad (1)
$$

$$
\begin{cases}
\dfrac{\partial W_{P11\_in}}{\partial t} = \dfrac{\partial W_{P11\_out}}{\partial t} \\
\dfrac{\partial W_{P21\_in}}{\partial t} = \dfrac{\partial W_{P21\_out}}{\partial t} \\
\dfrac{\partial W_{P0\_in}}{\partial t} = \dfrac{\partial W_{P0\_out}}{\partial t} \\
\dfrac{\partial W_{P12\_in}}{\partial t} = \dfrac{\partial W_{P12\_out}}{\partial t} \\
\dfrac{\partial W_{P22\_in}}{\partial t} = \dfrac{\partial W_{P22\_out}}{\partial t} \\
\dfrac{\partial W_{Pc1\_in}}{\partial t} = \dfrac{\partial W_{Pc1\_out}}{\partial t} \\
\dfrac{\partial W_{Pc1\_in}}{\partial t} = \dfrac{\partial W_{Pc1\_out}}{\partial t}
\end{cases}
\quad (2)
$$

2.2.Heat Transfer Models

To simulate the physical process in CEFR, a series of control volumes were used to describe the pool type PCS. The number and the distribution of these control volumes are the key focus for the accuracy and efficiency. The number should be few enough to keep the demand on real time computing, and the distribution should be reasonable to reflect the heat transfer.

To save the number, the detailed temperature difference was avoided for the hot/cold pools. So there is one assumption that the sodium from the outlet of reactor core can mix fully with the sodium in the hot pool, and the sodium from the outlet of IHX can mix fully with the sodium in the cold pool. In addition, the core and IHX are the key regions for heat transfer. To keep the accuracy, most of the control volumes were created for these regions rather than the cold/hot pools. So 22 control volumes were used to describe the core, especially 10 control bodies were set in the active region (0.45m in height). 30 control volumes were used in each IHX. The details for the distribution of the control volumes is shown in FIG. 3. The detailed description of the control volumes are listed in TABLE I.

TABLE I: DETAILS OF THE CONTROL VOLUMES

ID	Control volumes	ID	Control volumes
1	Argon region: 1 volume (001)	8	2# Primary pump: 27 volumes (075~077, 408~431)
2	Hot sodium pool: 8 volumes (002~005, 099~102)	9	Pressure chamber: 3 volumes (078~080)
3	1# IHX: 120 volumes (006~035, 144~233)	10	Reactor core: 108 volumes (081~098, 104~143, 451~500)
4	1# Cold sodium pool: 3 volumes (036~038)	11	Public region of reactor vessel cooling system: 1 volume (103)
5	1# Primary pump: 27 volumes (039~041, 384~407)	12	1# primary vessel cooling regions: 36 volumes (324~353, 432~436, 443)
6	2# IHX: 120 volumes (042~071, 234~323)	13	2# primary vessel cooling regions: 36 volumes (354~383, 437~442)
7	2# Cold sodium pool: 3 volumes (072~074)	14	Independent heat transfer: 20 volumes (444~450, 501~513)

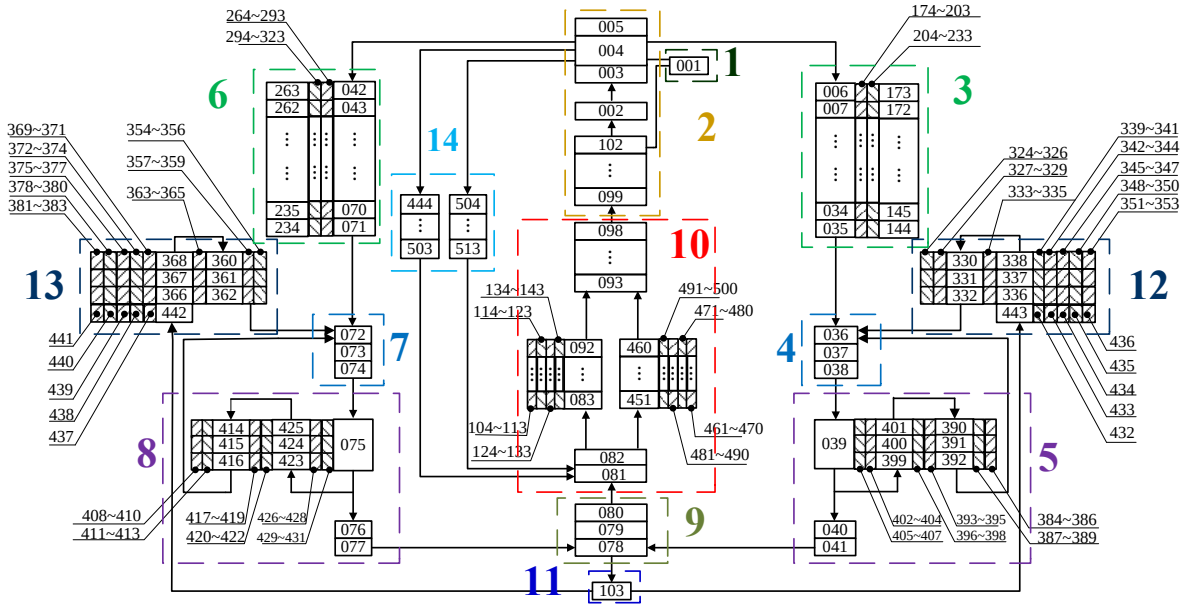

FIG. 3. The control volumes for the simulation of PCS in CEFR

To solve the fluid enthalpy and wall temperature, the energy conservation equations corresponding to the control volumes in FIG. 3 should be used. Then the heat transfer equation set is composed by 513 non-linear ordinary differential equations as the introduction of the following part.

2.2.1.Heat Transfer in the Core

In order to reflect the temperature distributions in fuel, cladding and coolant, an equivalent channel is defined by surrounding the fuel rod with an equivalent concentration of flowing sodium. The mathematical model of the rod-shaped fuel pellet, the cladding and coolant can be written as:

$$\rho_u c_u \frac{\partial T_u(r,t)}{\partial t} = \frac{1}{r}\frac{\partial}{\partial r}\left(\lambda_u r \frac{\partial T_u(r,t)}{\partial r}\right) + q_v \quad (3)$$

$$\rho_c c_c \frac{\partial T_c(r,t)}{\partial t} = \lambda_c \left[\frac{\partial^2 T_c(r,t)}{\partial r^2} + \frac{1}{r}\frac{\partial T_c(r,t)}{\partial r}\right] \quad (4)$$

$$\rho_{Na} c_{Na} A_{Na} \frac{\partial T_{Na}}{\partial t} = 2\pi r_c h\left(T_c - T_{Na}\right) - W c_{Na} \frac{\partial T_{Na}}{\partial z} \quad (5)$$

Where subscripts *u*, *c* and *Na* mean the fuel, the cladding, and coolant, respectively. *h* is the convective heat transfer coefficient between the cladding and coolant, which is a function of sodium temperature [7]. In these models, the axial conduction heat transfer along the height is neglected.

2.2.2.Heat Transfer in IHX

In the simulation for CEFR, IHX was modeled by a lumped parameter single tube model. The lumped parameter single tube model assumes that all the tubes behave identically, and hence an average tube represents all the tubes. Then IHX is radially treated as primary sodium (shell side), primary side of tube, secondary side of tube, secondary sodium and axially divided into 30 control volumes as shown in FIG. 4.

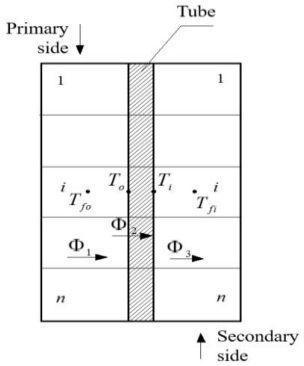

FIG. 4. Heat transfer and control volumes of IHX

Based on the energy balance and the heat transfer in the control volumes, a set of coupled partial differential equations are given as:

$$A_P \rho_P c_P \frac{\partial T_P}{\partial t} = c_P W_P \frac{\partial T_P}{\partial z} - A_P h_P \left(T_P - T_1\right) \quad (6)$$

$$\left(mc\right)_1 \frac{\partial T_1}{\partial t} = -KA\frac{\partial T_{12}}{\partial x} + h_1 A_1 \left(T_P - T_1\right) \quad (7)$$

$$\left(mc\right)_2 \frac{\partial T_2}{\partial t} = KA\frac{\partial T_{12}}{\partial x} - h_2 A_2 \left(T_2 - T_S\right) \quad (8)$$

$$A_S \rho_S C_S \frac{\partial T_S}{\partial t} = A_2 h_2 \left(T_2 - T_S\right) - c_S W_S \frac{\partial T_S}{\partial z} \quad (9)$$

Where subscripts *P*, *1*, *2*, and *S* refer to primary sodium (shell side), primary side of tube, secondary side of tube, and secondary sodium, respectively.

2.2.3.Heat Transfer in Hot/Cold Pool

The hot pool receives the sodium from various assemblies at different temperatures. The mixing process in the hot pool is characterized by a mathematical model as below.

$$(mC_P)_1 \frac{\partial T_1}{\partial t} = \sum_{i=1}^{N} W_i(t) C_{Pi}(t)\left(T_i(t) - T_1(t)\right) \qquad (10)$$

Where T_1 is the mixed mean temperature of hot pool sodium, *i* represents various streams of sodium from the different assemblies. Sodium exiting from IHX enters the cold pool, where it mixes with the resident sodium. The process is also characterized by this numerical scheme as same as the hot pool.

2.3.Solution Scheme

The dynamic characteristics of PCS is obtained by the solution of the equations for heat transfer and flow distribution. The thermal condition is related to the solution of the heat transfer equation set, and Gear method [8] is used to solve these equations. Gear method is designed especially for the stiff equation system, but this method needs much time for the iteration if there are too many equations. To ensure the solution efficiency, the flow equations were not solved together by the same numerical method. The flow distribution is related to the solution of Eq.1 and Eq.2, and Quasi-Newton method is used to solve these equations to obtain the flow status. Then the simulation results reflecting the coolant flow status and heat transfer status were exchanged at each time step. In addition, these solving processes have been transplanted on the real-time simulation platform SIMSEXE to achieve the control of the solution efficiency and data transfer.

3 Validation and Analysis

TABLE II: VALIDATION AND ANALYSIS FOR STEADY-STATE CONDITONS

Variables	Relative Error based on the values of design conditions / %					
	100% FP	75% FP	60% FP	50% FP	40% FP	26.5% FP
Core coolant flow rate (kg/s)	0	0.004	0.015	0.105	0.076	0.152
Coolant temp. at the inlet of core (℃)	1.269	1.181	1.130	1.079	0.989	0.761
Coolant temp. at the outlet of core (℃)	0.100	0.224	0.214	0.108	0.090	0.114
Flow rate at the primary side of IHX (kg/s)	0.006	0.008	1.394	1.696	2.158	2.198
Flow rate at the secondary side of IHX (kg/s)	0	0	0	0	0	0
Coolant temp. at the inlet of the primary side of IHX (℃)	0.120	0.305	0.305	0.248	0.269	0.322
Coolant temp. at the outlet of the primary side of IHX (℃)	0.603	0.817	0.896	0.963	1.055	0.711
Coolant temp. at the inlet of the secondary side of IHX (℃)	0	0	0	0	0	0
Coolant temp. at the outlet of the secondary side of IHX (℃)	0.325	0.023	0.057	0.028	0.074	0.206

In the following validation and analysis, the simulation results are compared with design values and the data in the final safety analysis report of CEFR [9].

3.1. Steady State Condition

The design parameters of CEFR were used to validate six different steady-state conditions from 26.5%FP to 100%FP by this code. As the comparison in TABLE II, the steady simulation is high accurate especially for the conditions with high power.

3.2. Normal Operational Condition

In CEFR, the normal operational conditions contain the shutdown condition, power operation, start/shut-down operation, maintenance, test, refueling, etc. In these operational conditions, shut-down operation is one key and complex process, therefore it was chosen to validate the simulation code. In the validation, the shut-down operation was calculated and compared with the manual of PCS of CEFR, as shown in FIG. 5~FIG. 7. It can be found that the trends can be reflected well for the key physical parameters. In addition, the reference values did not consider the thermal inertia of the hot & cold sodium pools which contains 260 tons of sodium. The temporal deviation was created in FIG. 6 and FIG. 7, because the thermal inertia has been modeled in the cold pool for CEFR.

3.3.Accident Condition

3.3.1.The Reactivity Insertion Accident

This kind of accident is caused by a sudden insertion of a positive reactivity which results in the power increases over the set point. This accident is dangerous enough to damage the integrity of PCS. Hence, it has been the research focus, and the transient overpower has already been analyzed in our previous researches [10,11]. In this paper, the accident caused by the cold sodium was analyzed. Due to the negative feedback effect, cold sodium can cause a positive reactivity. In the simulation, the two primary pumps have a simultaneous acceleration when the core is operating at the 40% FP. As shown in FIG. 8~FIG. 10, the system's transient response characteristics have been computed and compared with the data in final safety analysis report. The comparison shows that the trend and the values of each key parameter agrees well with the data in safety report. So the feasibility can be satisfied well for this kind accident.

3.3.2.The Loss of Coolant Accident

As a design basis accident in sodium cooled fast reactor, loss of flow may be initiated due to loss of AC power (LOOP), loss of primary pumps and abnormal closure of primary valves. The last two conditions have been analyzed in our previous work [12]. The loss of the coolant accident caused by the station blackout is mainly calculated and analyzed in this paper. As shown in FIG. 11~FIG. 13, the system's transient response characteristics have been computed and compared with the data in final safety analysis report. The comparison shows that the trends and the values of each key parameter agrees well with the data in the safety report.

3.3.3.The Loss of Heat Sink Accident

In CEFR, the secondary and the tertiary circuit is heat sink of the primary circuit. If the secondary or the tertiary circuit can't operate normally, the heat removal is then retained in the primary circuit. So sodium temperature in the primary circuit will rise. Loss of heat sink accident is formed. The reactor is operating under rated conditions previously. After initiation of the accident, the secondary pump in loop1 is tripped and begins to operate by the drive inertia of flywheel. Results of this simulation are presented in FIG. 14~FIG. 16, which show the results from DINROS code and the code presented in this paper. The comparison results show that the trends of these curves agree well with each other.

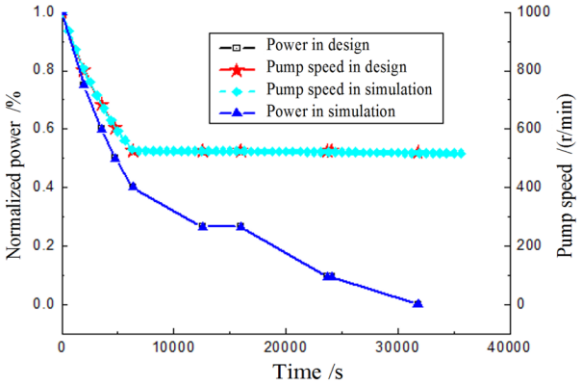

FIG. 5. The power and pump speed under the shut-down operation

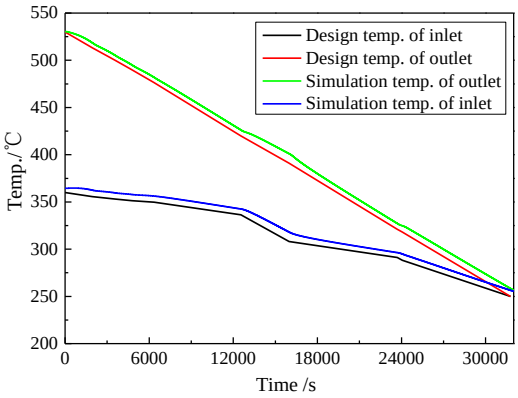

FIG. 6 Temp. at reactor core inlet/outlet

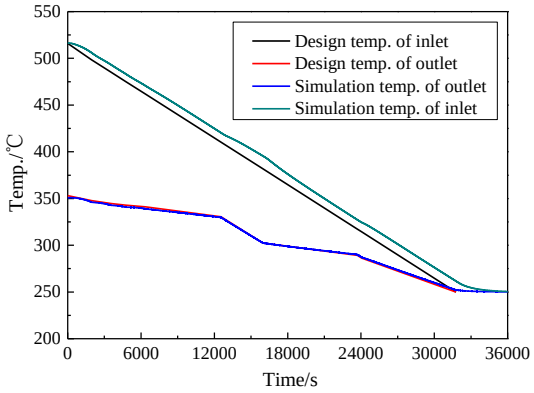

FIG. 7 Temp. at the inlet/outlet of the primary side of IHX

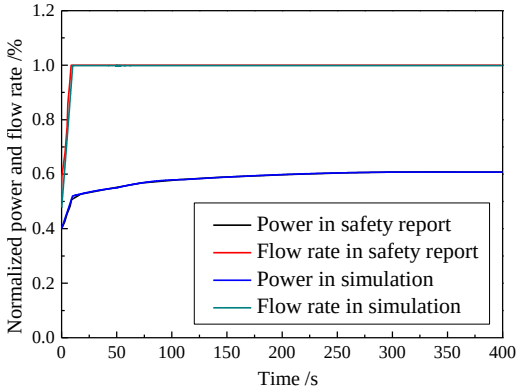

FIG. 8 Variations of power and flow rate

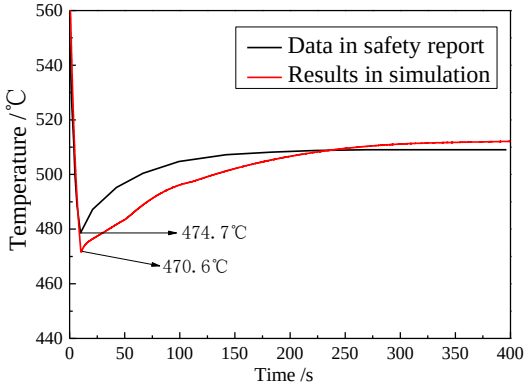

FIG. 9 The coolant temp. of the core outlet

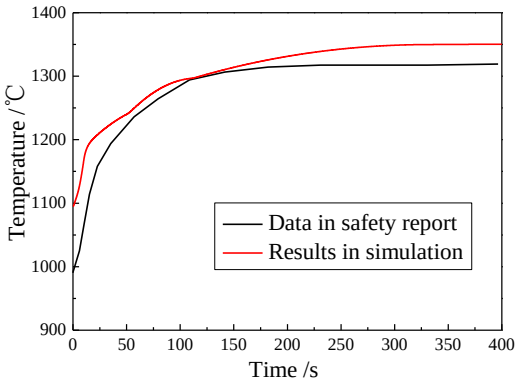

FIG. 10 The maximum fuel temp.

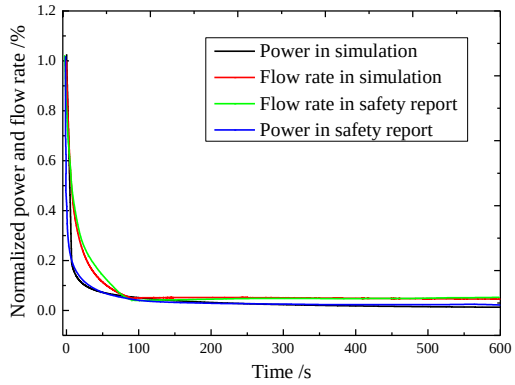

FIG. 11 Variations of power and flow rate

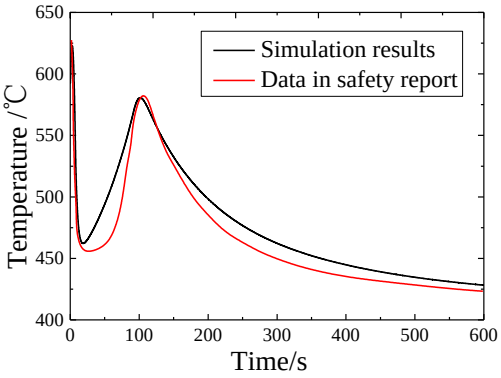

FIG. 12 The coolant temp. at the core output

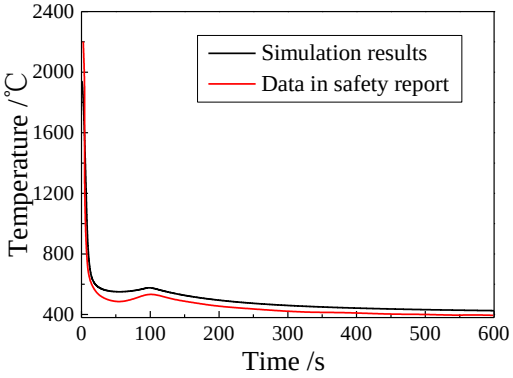

FIG. 13 The maximum fuel temp.

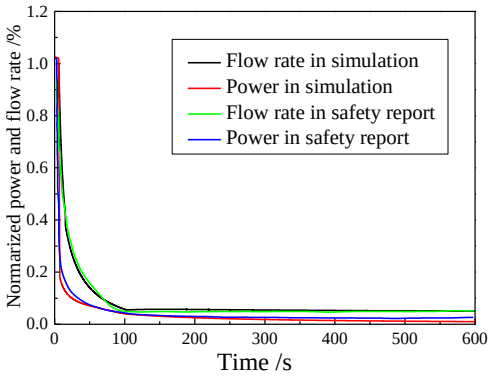

FIG. 14 Variations of power and flow rate

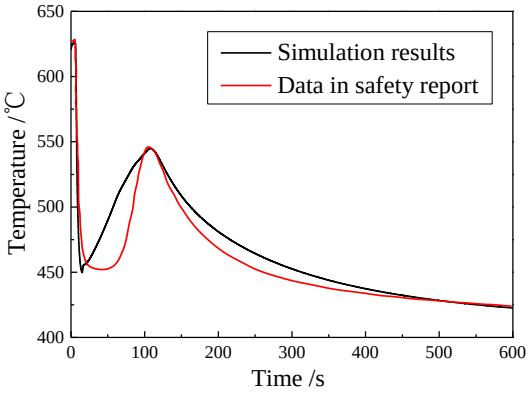

FIG. 15 Coolant temperature at the core output

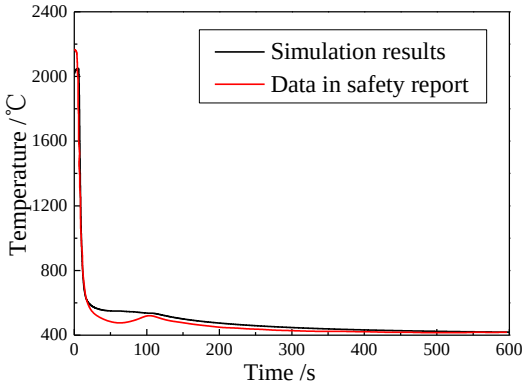

FIG. 16 The maximum fuel temperature

3.4.Efficiency Analysis

The simulation will cost more time if it is used for a high transient condition. Hence, the accident analysis needs more computing time. To test the real-time ability of this developed code, three simulations for accident conditions have been analyzed.

TABLE III: EFFICIENCY ANALYSIS FOR ACCIDENT CONDITIONS

Case	CPU time /s	Simulation time /s	Ratio (CPU time/ simulation time)
Evnet (3.3.1)	100	400	0.25
Event (3.3.2)	185	600	0.31
Event (3.3.3)	175	600	0.29

As shown in TABLE III, all the simulations can realize the real-time simulation. In addition,

the analysis was just based on a PC with a 1.87 GHz Intel CORE Duo processor and 4GB computer memory. So the computing efficiency of this code is really enough for CEFR.

4 Conclusions

In this work, detailed models for heat transfer and fluid flow in sodium cooled pool type PCS of CEFR have been built. The trends of the main parameters in different conditions have been compared with the design values and the data of the safety analysis report. The results showed that the steady and transient simulations are reasonable and accurate. The efficiency analysis on the computing ability has also been provided, and the real-time characteristics of the code could satisfy the simulation requirements.

REFERENCES

[1] ALBRIGHT, D.C., BARI, R.A. “Primary pipe rupture accident analysis for Clinch River breeder reactor plant”. Nucl. Technol. 39 (3), 225–257, (1978).

[2] ALLISTON, W.H. “Clinch River Breeder Reactor Plant: LMFBR Demo Plant Simulation Model (DEMO)”. Westinghouse Electric Corporation, Report, (1978）.

[3] MOHR, D., FELDMAN, E.E. “A dynamic simulation of the EBR-II plant with the NATDEMO Code”. In: Agrawal, A., Guppy, J. (Eds.), Decay Heat Removal and Natural Circulation in Fast Breeder Reactors. Hemisphere Publishing Co., Washington, DC. (1981) 207–224.

[4] AGRAWAL, A.K. “An Advanced Thermo-hydraulic Simulation Code for Transients in LMFBRs (SSC-L Code)”. BNL-NUREG-30773, (1978).

[5] CHANG, W.P., KWON, Y.M., LEE, Y.B., et al. “Model development for analysis of the Korea advanced liquid metal reactor”. Nucl. Eng. Des. 217, 63–80, (2002).

[6] LEE, Y.B., CHANG, W.P., KWON, Y.M., et al. “Development of a two-dimensional model for the thermo hydraulic analysis of the hot pool in liquid metal reactors”. Ann. Nucl. Energy 29, 21–40, (2002).

[7] AOKI, S. “Current liquid metal heat transfer in Japan”, Progress in heat and mass transfer, Vol. 7, 569-587, (1973).

[8] GEAR, A.C. “Ordinary Differential Equation System Solver. Lawrence Livermore Laboratory”, Report UCID-30001. Revision 3, December, (1974).

[9] YANG, F.C., XIE, G.S., LI, Z.H., et al. “The Final Safety Analysis Report of Chinese Experimental Fast Reactor”. China Institute of Atomic Energy, (2008).

[10] CUI, M., GUO, Y., ZHANG, Z. “Transient simulation code development of primary coolant system of Chinese Experimental Fast Reactor”. Annals of Nuclear Energy, 53 (2013) 158–169.

[11] CUI, M., GUO, Y., ZHANG, Z. “Simulation on primary coolant system of sodium cooled fast reactor”. 19th International Conference on Nuclear Engineering. Chiba, Japan, May 16-19, (2011).

[12] Yu, Y., Guo, Y. “Dynamics simulation research on primary coolant system of sodium cooled fast reactor”. Proceedings of the 2012 20th International Conference on Nuclear Engineering. Anaheim, California, USA, (2012).